Optical Observations of the Second Russian Earth Satellite

AUTHOR(S):

Hattori, Akira; Yada, Bunta

CITATION:

Hattori, Akira ...[et al]. Optical Observations of the Second Russian Earth Satellite. Memoirs of the College of Science, University of Kyoto. Series A 1959, 29(2): 107-139

ISSUE DATE:

1959-09

URL:

http://hdl.handle.net/2433/257424

Memoirs of the College of Science, University of Kyoto, Series A,
Vol. XXIX, No. 2, Article 1, 1959.

OPTICAL OBSERVATIONS OF THE SECOND RUSSIAN EARTH SATELLITE

BY

Akira HATTORI* and **Bunta YADA***

(*Received August 27, 1958*)

ABSTRACT

This paper deals with the observations of 1957β carried out at Kwasan Observatory and in cooperation with the Western Japanese Moon Watch Stations. Part I gives the description of instruments used and observational data. In part II, the orbital elements are determined. For example, on March 20.000 (J.S.T.), 1958, the period T was $94.^{m}477 \pm 0.^{m}003$, the eccentricity 0.0434 ± 0.0020, and perigee and apogee heights were 195 km$\pm$14 km and 791 km$\pm$14 km respectively. The inclination of orbit to the equatorial plane, i, is estimated as $65.^{\circ}5 \pm 0.^{\circ}2$. In part III, some results are derived. The period shows erratic variations. $\Delta\Omega$, the retrograde rate of orbit per day, may be connected with the period by an empirical formula: $\Delta\Omega = (1.08 \pm 0.01) \times 10^{5} \cos i \times T^{-2.1 \pm 0.1}$. Finally, air density at about 195 km altitudes above the equatorial regions is estimated as 6×10^{-10} kg m^{-3} to 10×10^{-10} kg m^{-3}.

I. OBSERVATIONS

1. Introduction

It is well known that the calculation of air density from the measured drag of a satellite is one of the frequently suggested uses of the vehicle. Especially, above about 200 km there are no direct determinations of air density or pressure, and air density must be computed from an assumed temperature and molecular weight. But, considering the observations of the satellite orbit, we can evaluate the atmospheric density roughly in the order of magnitude.

In July 1955, the announcement of the American program for the launching of small satellites during the International Geophysical Year was made. Soon after the Russian authorities announced that they were also undertaking the same plan. At Kwasan Observatory, it was planned to observe Earth satellites for the study of physical conditions of the upper atmosphere. So, we started at once to construct Schmidt cameras. In spring 1956 a 16 cm F 1.5 camera was built, and in September 1957 a 40 cm F 1.5 camera was completed. On October 4, the U.S.S.R. announced from Moscow the

* Kwasan Observatory, Kyoto University.

launching of the first Earth satellite (1957 α). We immediately began to observe the satellite by the two Schmidt cameras. The first photographs were obtained on the morning of October 16. At about a month after the launching of the first, the news of the launching of the second Earth satellite (1957 β) was received. At that time, the Baker Schmidt camera had not arrived yet at Tokyo Observatory. As a Schmidt camera of medium size in Japan, our 40 cm camera was the only available one.

In this paper we deal with 1957 β only. According to the preliminary reports from Moscow, it was launched on the morning of November 3, weighing 508.3 kg, moving in an elliptic orbit with its maximum altitude of 17000 km, and taking about 103.7 minutes to complete one revolution. It was also reported that the satellite was travelling in an orbit inclined at about 65° to the equatorial plane.

At Kwasan, the observations of 1957 β were carried out from November 6, 1957 to March 21, 1958. The Moon Watch teams in Western Japan — Shizuoka, Yokkaichi, Kashiwara, Osaka, Kanaya, Tadotsu, Kochi, Hiroshima and Miyazaki (including photographs) — also reported their observational data to us. By adding these to ours, the orbital elements of the satellite and their variations have been determined. Using these values, we have derived an empirical formula between the retrograde rate of orbit and the period, and have finally estimated the air density at perigee altitudes.

2. Observations

a) *Instruments*

The observational material mainly consists of a group of Kwasan 40 cm F 1.5 Schmidt (film diameter 10 cm, field 8°, designed by Y. Nakai) and 16 cm F 1.5 Schmidt (film diameter 6 cm, field 15°) photographs taken by Y. Nakai, S. Saito and the present authors and of a number of photographs obtained by the present authors with a Nikon S II camera (F 1.2). We used the exposure time of 2~10 seconds. Fuji SSS film and Fuji X-Ray film for fluorography were used. All films were developed with Rendol at 20°C (3 minutes for SSS, 6 minutes for X-Ray film).

In order to record the time at which the shutters were opened and closed, three methods were adopted; 1. synchronized recording of shutter signals and J.J.Y. signals from radio into pen-oscillograph, 2. synchronized recording of the two signals into tape-recorder, 3. eye and ear methods with a chronometer. The instruments we have made use of are illustrated in Figs. 1 a, 1 b and 1 c. Moon Watch teams used Astro and Nikko Satellite telescopes (field 7°). Time recordings were made by using tape-recorder and J.J.Y. signals. Miyazaki Team took also many photographs.

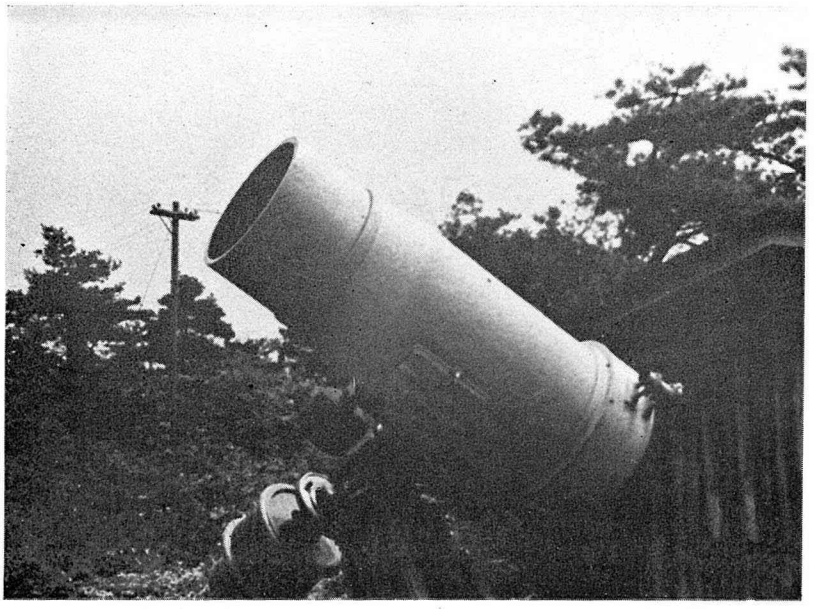

Fig. 1 a. 40 cm Schmidt camera.

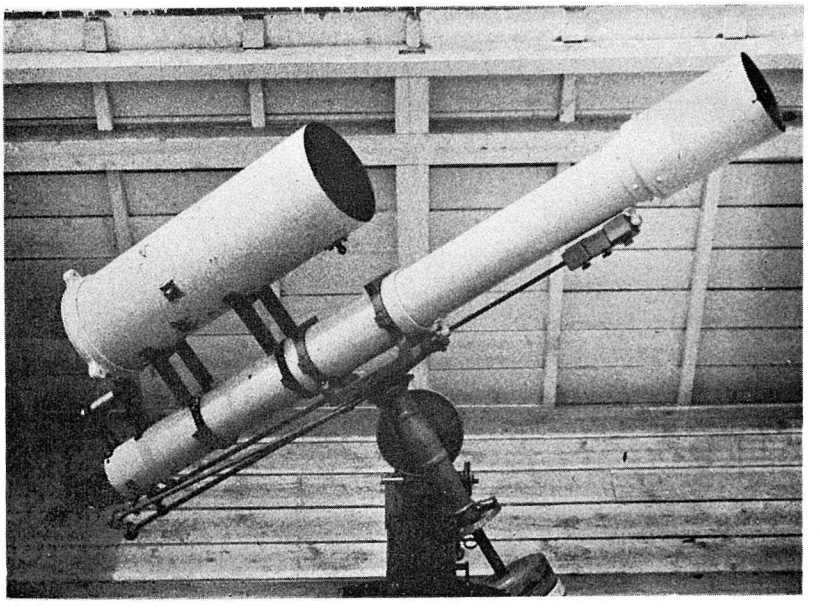

Fig. 1 b. 16 cm Schmidt camera.

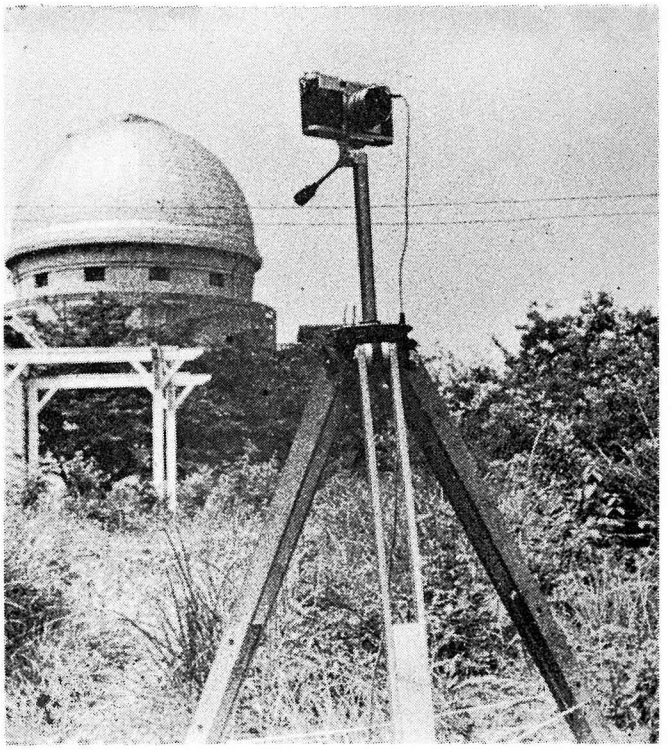

Fig. Ic. Nikon S II camera.

b) *Data*

Observations of the satellite consist in measuring its position at a recorded time. As for the photographic observation, the time recorded is that of the opening or closing of the shutters. Fig. 2 shows an example of the photographic observation.

Table 1.

No.	Team	Longitude	Latitude	Altitude
1	Shizuoka	138°23′18″E	34°58′25″N	20 m
2	Yokkaichi	136 39 00	35 00 15	3
3	Kashiwara	135 48 15	34 30 24	66
4	Kwasan	135 47 33.66	34 59 55.46	221
5	Osaka	135 30 30	34 41 51	30
6	Kanaya	135 15 10	34 03 46	40
7	Tadotsu	133 45 16	34 16 20	2–5
8	Kochi	133 30 35	33 33 25	30
9	Hiroshima	132 28 10	34 22 08	3
10	Miyazaki	131 25 24	31 55 23	8

Fig. 2 a. A photograph taken by the 16 cm Schmidt camera: the left end of the trail corresponds to the current number 188 in Table 2, and the right end to 189.

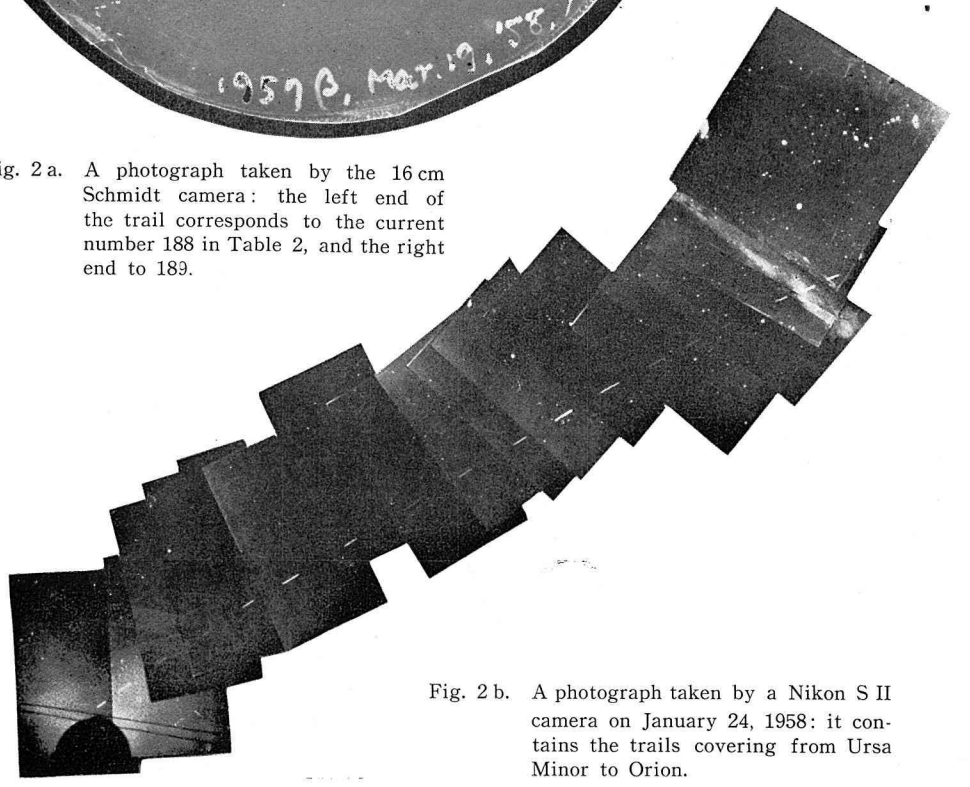

Fig. 2 b. A photograph taken by a Nikon S II camera on January 24, 1958: it contains the trails covering from Ursa Minor to Orion.

Table 2.

No.	Date	Team	Time	R.A.	Declination	Azimuth	Altitude	Remarks
			h m s	h m				
1	Nov. 6, '57	Kochi	5 8 16	8 2	−43°	S 0° 6′E	13°27′	V.
2		Shizuoka	5 9 25.5	6 50	−29	S21 44W	22 26	V.
3		Kwasan	~5 10 50.0	—	—	~E	—	P.*
4	Nov. 7, '57	Kwasan	5 21 20.2	5 21.8	+18.25	S80 13W	45 42	P.
5			21 39.00	5 18	+45.1	N59 29W	52 51	P.
6			21 43.32	5 17	+49.5	N52 14W	52 33	P.
7			21 46.75	5 16.3	+52.3	N47 42W	52 8	P.
8			21 50.12	5 15	+57.3	N39 51W	51 0	P.
9			22 24.68	19 30	+84.46	N 1 37E	29 38	P.
10			22 28.48	18 41	+82.25	N 3 58E	28 2	P.
11			22 33.25	18 30	+79.58	N 5 43E	25 49	P.
12			22 37.83	18 18	+77.34	N 7 28E	24 7	P.
13			22 59.83	18 3	+68.7	N13 6E	17 11	P.
14			23 13.77	18 2	+66.0	N14 38E	14 55	P.
15			23 17.95	18 1	+65.2	N15 9E	14 17	P.
16		Shizuoka	5 21 33.0	4 2	+25	N79 15W	30 31	V.
17	Nov. 8, '57	Kanaya	5 33 27	—	—	N 5 W	8	V.
18		Hiroshima	5 33 39	19 45	+62	N 5 22E	6 48	V.
19	Dec. 9, '57	Shizuoka	5 18 5	17 55	+51.3	N38 12E	16 32	V.
20	Dec. 10, '57	Shizuoka	5 5 56	17 30	+50	N40 54E	17 58	V.
21	Dec. 12, '57	Kwasan	6 24 40	—	—	~N40 W	~40	P.§
22	Dec. 13, '57	Kanaya	6 11 3	10 35	+20	S48 25W	70 18	V.
23	Dec. 14, '57	Kanaya	5 55 58	10 35	+20	S42 5W	71 57	V.
24		Yokkaichi	5 55 59	10 8	+14	S47 7W	61 48	V.
25		Kochi	5 56 18	11 34	+15	S10 59E	71 9	V.

Table 2. (continued)

No.	Date	Team	Time	R.A.	Declination	Azimuth	Altitude	Remarks
			h m s	h m				
26	Dec. 15, '57	Kwasan	5 39 14.5	9 12	+33.°6	N84°14′W	64°34′	P.
27			39 19.5	9 19	+32.3	N88 1W	65 43	P.
28		Yokkaichi	5 40 19	10 4	+13	S 42 39W	62 6	V.
29	Dec. 16, '57	Kwasan	5 22 23	8 23	+43.4	N62 26W	58 19	P.
30			22 27	8 33	+42.1	N64 54W	60 10	P.
31			24 2	10 28	+10.8	S 20 55W	64 27	P.
32			24 6	10 33	+ 9.2	S 17 17W	63 14	P.
33		Kashiwara	5 23 18	9 51	+27	S 69 6W	72 46	V.
34		Kanaya	5 23 50	10 26	+20	S 31 40W	73 52	V.
35		Yokkaichi	5 23 56	10 8	+13	S 35 3W	64 15	V.
36		Miyazaki	5 25 34	12 56	− 3	S 47 2E	43 44	V.
37		Kochi	5 27 11	12 36	−24	S 25 21E	27 55	V.
38		Kanaya	5 27 37	12 18	−26	S 18 22E	27 31	V.
39	Dec. 17, '57	Kwasan	5 4 57	7 59	+48.8	N52 48W	56 3	P.
40			5 7	8 17	+47.0	N55 18W	59 16	P.
41			6 37	10 16	+16.8	S 25 12W	70 14	P.
42			6 46	10 23	+13.5	S 17 57W	67 37	P.
43	Dec. 18, '57	Miyazaki	4 50 42	12 45	− 1	S 53 0E	42 38	V.
44	Dec. 19, '57	Kwasan	4 33 43	11 43	−17.8	S 22 26E	34 5	P.
45			33 55	11 46	−19.8	S 22 23E	31 59	P.
46	Dec. 23, '57	Miyazaki	17 52 31	1 55	+29	N87 22E	61 53	V.
47		Hiroshima	17 52 38	23 49	−11	S 0 10W	44 38	V.
48		Shizuoka	17 53 7	19 47	+12.5	S 87 6W	26 15	V.
49		Yokkaichi	17 53 24	20 19	+39	N67 19W	45 8	V.
50		Osaka	17 53 49	23 59	+89	N 0 1W	35 42	V.

Table 2. (continued)

No.	Date	Team	Time	R.A.	Declination	Azimuth	Altitude	Remarks
			h m s	h m				
51	Dec. 24, '57	Kanaya	17 30 2	0 5	+18°	S19°36′E	73° 7′	V.
52		Kashiwara	17 30 59	6 10	+59	N34 43E	26 1	V.
53	Jan. 23, '58	Kashiwara	19 17 3	18 40	+63	N20 18W	14 39	V.
54		Osaka	19 19 59	2 0	+64	N18 25W	57 34	V.
55			22 9	4 33	+16	S39 23E	67 0	V.
56		Kanaya	19 21 2	3 53	+46	N17 40E	77 22	V.
57			21 59	4 40	+24	S60 16E	72 5	V.
58		Miyazaki	19 21 23	6 13	+45.0	N56 2E	53 30	V.
59		Yokkaichi	19 22 41	4 34	+ 7	S27 50E	59 12	V.
60			22 45	4 35	+ 5	S26 48E	57 17	V.
61	Jan. 24, '58	Kwasan	18 24 18	15 50	+72	N 5 35W	17 42	P.
62			24 24	15 43	+73	N 4 47W	18 32	P.
63			24 44	15 31	+74.8	N 3 29W	20 7	P.
64			24 50	15 15	+76.4	N 2 9W	21 32	P.
65			25 1	14 29	+78.5	N 0 39E	23 31	P.
66			25 10	14 5	+79.5	N 1 48E	24 37	P.
67			25 27.5	12 43	+80.8	N 5 5E	26 53	P.
68			25 33	12 15	+81.0	N 6 3E	27 38	P.
69			25 51	10 13	+80.0	N10 43E	30 39	P.
70			25 58	9 48	+79.5	N11 49E	31 26	P.
71			26 12.5	8 49	+77.0	N15 40E	33 36	P.
72			26 19.5	8 28	+75.4	N17 48E	34 36	P.
73			26 39	7 47	+70.5	N24 3E	37 19	P.
74			26 44	7 38	+69.8	N24 55E	38 6	P.
75			27 6.5	7 13	+62.2	N34 42E	40 49	P.

Table 2. (continued)

No.	Date	Team	Time	R.A.	Declination	Azimuth	Altitude	Remarks
			h m s	h m				
76	Jan. 24, '58	Kwasan	18 27 11.5	7 8	+60.°6	N36°49′E	41°27′	P.
77			27 25	7 0	+56.3	N42 37E	42 29	P.
78			27 30	6 57	+54.3	N45 21E	42 50	P.
79			27 48	6 47	+48.8	N53 5E	44 0	P.
80			27 53	6 46	+47.2	N55 19E	44 0	P.
81			28 4.5	6 44	+43.2	N60 53E	43 44	P.
82			28 9.5	6 42	+41.0	N63 58E	43 40	P.
83			28 22.5	6 39	+37.2	N69 15E	43 19	P.
84			28 30	6 37	+34.0	N73 37E	42 47	P.
85			28 49	6 33	+28.6	N80 53E	41 45	P.
86			28 58	6 33	+25.6	N84 32E	40 32	P.
87			29 5	6 32	+23.6	N87 3E	39 53	P.
88			29 14	6 32	+21.2	N89 48E	38 49	P.
89			29 20	6 31	+20.1	S88 48E	38 30	P.
90			29 14	6 31	+21.2	N89 57E	39 1	P.
91			29 20	6 30.5	+20.0	S88 37E	38 33	P.
92			29 43	6 29	+13.7	S81 35E	35 38	P.
93			29 48	6 28	+12.3	S79 59E	35 6	P.
94			29 59	6 28	+10.4	S78 3E	34 2	P.
95			30 3	6 27	+ 9.8	S77 17E	33 54	P.
96			30 10	6 27	+ 7.5	S75 3E	32 33	P.
97			30 17	6 27	+ 5.8	S73 26E	31 33	P.
98		Shizuoka	18 26 2	2 49	+85	N 0 6W	39 59	V.
99		Miyazaki	18 26 33	8 55	+64.6	N28 6E	25 29	V.
100			27 17.0	8 21.4	+53.3	N41 32E	25 42	V.

Table 2. (continued)

No.	Date	Team	Time	R.A.	Declination	Azimuth	Altitude	Remarks
			h m s	h m				
101	Jan. 24, '58	Miyazaki	18 28 49.8	7 32	+32.°2	N67°12′E	26°58′	V.
102		Osaka	18 28 7	6 46	+43	N60 45E	43 0	V.
103			32 24	6 28	−13	S57 55E	19 14	V.
104		Yokkaichi	18 28 13	6 36	+44	N60 16E	45 56	V.
105		Kanaya	18 28 43	6 52	+34	N71 21E	39 11	V.
106		Miyazaki	20 8 45.5	0 7.6	+27.6	N78 19W	38 25	V.
107			9 20.4	0 36.6	+20.8	N89 46W	41 48	V.
108			9 25.9	0 44	+19.2	S87 18W	42 40	V.
109			9 48.0	1 1	+14.6	S79 8W	43 59	V.
110			10 29.0	1 37.5	+ 5.5	S61 23W	45 49	V.
111		Kashiwara	20 8 49	23 59	+12	S86 51W	26 2	V.
112	Jan. 25, '58	Kwasan	19 14 49	0 36	+33	N79 59W	53 11	P.
113			14 58.5	0 43	+31.7	N82 46W	54 13	P.
114			15 4.5	0 50	+30	N86 22W	55 4	P.
115			15 8.5	0 54	+28.4	N89 31W	55 20	P.
116			15 4.5	0 49	+30.1	N86 5W	54 54	P.
117			15 8.5	0 54	+29.1	N88 22W	55 34	P.
118			16 23	2 13.5	+ 7.3	S39 22W	56 23	P.
119			16 27.5	2 17.5	+ 6.0	S36 40W	55 45	P.
120			16 36.5	2 25	+ 3.8	S32 3W	54 39	P.
121			16 42	2 28	+ 2.5	S29 58W	53 47	P.
122			16 47	2 36	− 0.5	S25 4W	51 46	P.
123			16 57	2 40	− 1.5	S23 6W	51 9	P.
124		Kashiwara	19 15 4	24 48	+32	N82 6W	55 13	V.
125			16 54	2 35	+ 1	S26 41W	53 30	V.

Table 2. (continued)

No.	Date	Team	Time	R.A.	Declination	Azimuth	Altitude	Remarks
			h m s	h m				
126	Jan. 25, '58	Kashiwara	19 18 57	3 43	−23°	S 1°4′ E	32°30′	V.
127		Kanaya	19 15 11	0 56	+34	N78 49W	57 40	V.
128			15 57	1 52	+19	S62 51W	62 49	V.
129			16 55	2 40	+ 3	S25 19W	56 25	V.
130			18 8	3 32	−15	S 1 17W	40 55	V.
131			19 9	3 59	−24	S 5 54E	31 42	V.
132			20 25	4 30	−32.5	S11 45E	22 20	V.
133		Hiroshima	19 16 30	3 24	+ 9	S 0 25E	64 38	V.
134		Miyazaki	19 17 39.6	4 26	+ 1.3	S30 8E	55 40	V.
135			17 57.6	4 33	− 3.4	S29 21E	49 48	V.
136			19 39.9	5 4.4	−22.1	S27 41E	30 42	V.
137		Tadotsu	19 17 43	3 43	−10	S 4 43E	45 37	V.
138		Yokkaichi	19 18 39	3 29	−22	S 3 38W	32 55	V.
139	Jan. 27, '58	Miyazaki	19 4 23.0	22 28	+49.8	N48 34W	35 10	V.
140			4 27.9	22 36	+49.3	N49 26W	36 21	P.
141			5 6.5	23 30	+44.1	N57 32W	44 52	P.?
142			5 38.9	0 12	+37.6	N68 18W	52 9	P.?
143			6 3.5	0 42	+31.9	N79 33W	57 24	P.
144			6 8.0	0 47	+30.5	N82 31W	58 9	P.
145			8 30.1	2 48.2	− 9.9	S11 15W	47 32	V.
146			9 2.0	3 7	−16.3	S 4 1W	41 41	V.
147		Kanaya	19 4 35	22 8	+32	N66 38W	24 19	V.
148			4 38	22 52	+30	N73 12W	32 1	V.
149			5 4	23 8	+28	N77 1W	34 20	V.
150			5 32	23 36	+23	N85 53W	37 50	V.

Table 2. (continued)

No.	Date	Team	Time	R.A.	Declination	Azimuth	Altitude	Remarks
			h m s	h m				
151	Jan. 27, '58	Kanaya	19 6 14	0 15	+14°	S 78°8′W	41°19′	V.
152			7 13	1 46	−13	S 33 2W	36 30	V.
153		Yokkaichi	19 6 43	0 33	+ 4	S 64 51W	37 13	V.
154		Tadotsu	19 5 8	23 30	+28	N 79 30W	40 2	V.
155	Jan. 28, '58	Kobe	−18 9 25	—	—	—	−90	V.&
156	Jan. 30, '58	Yokkaichi	17 54 12	0 3	+27	S 87 7W	56 13	V.
157		Osaka	17 54 18	—	—	—	—	V.
158	Mar. 13, '58	Kashiwara	5 26 19	23 44	+60	N 31 54E	23 10	V.
159			29 53	21 38	+ 8	S 86 0E	19 57	V.
160	Mar. 14, '58	Miyazaki	5 18 30	22 27	+32	N 62 10E	16 26	V.?
161	Mar. 15, '58	Kanaya	5 3 10	21 30	+37	N 63 46E	30 54	V.?
162	Mar. 16, '58	Kanaya	4 50 41	21 6	+16	N 86 50E	24 42	V.
163	Mar. 17, '58	Kanaya	4 31 25	21 45	+49	N 47 58E	28 30	V.
164		Kashiwara	4 32 51	20 55	+25	N 78 0E	28 58	V.
165	Mar. 18, '58	Miyazaki	19 33 21±1	5 45	− 3	S 30 52W	50 42	V.
166			33 31.6	6 0.6	+ 5.8	S 31 37W	60 18	V.
167	Mar. 19, '58	Kwasan	3 52 41.4	21 12.40	+44.18	N 53 43E	27 55	P.
168			52 46.4	21 9.20	+43.20	N 55 0E	28 5	P.
169			54 17.4	20 31.25	+18.30	N 84 3E	24 21	P.
170			54 24.4	20 29.20	+16.40	N 86 7E	23 49	P.
171		Miyazaki	5 28 48	12 51	+46	N 54 29W	41 15	V.
172			28 54	12 58	+45.5	N 55 19W	42 24	P.
173			28 58.9	13 7	+44.1	N 57 25W	43 51	P.
174			30 34.1	15 24	+13.7	S 55 46W	61 30	P.?
175			31 58.4	16 39	−13.6	S 7 33W	44 10	P.?

Table 2. (continued)

No.	Date	Team	Time	R.A.	Declination	Azimuth	Altitude	Remarks
			h m s	h m				
176	Mar. 19, '58	Miyazaki	5 32 6.8	16 47.5	−16.°7	S 4°25′W	41°16′	P.?
177			32 11.7	16 51	−17.9	S 3 15W	40 15	P.
178			32 17.1	16 54	−19.2	S 2 17W	38 51	P.?
179		Kanaya	5 29 34	13 25	+17	S86 38W	36 18	V.
180		Miyazaki	19 11 28.3	6 0	−26	S11 18W	31 11	P.
181			12 5.6	7 31.2	+10.8	S30 7E	66 11	V.
182			13 1	11 52.1	+55.3	N41 22E	32 59	P.
183		Kochi	19 12 48	6 48	+34	N65 3W	88 56	V.
184		Tadotsu	19 12 50	6 30	+16.5	S18 6W	71 27	V.
185		Kashiwara	19 12 55	4 23	+15.4	S71 58W	49 36	V.
186			13 17	4 45	+47	N53 36W	61 27	V.
187		Yokkaichi	19 13 2	4 0	+12.0	S72 58W	42 14	V.
188		Kwasan	19 13 9.5	4 47.5	+24.8	S79 53W	59 16	P.
189			13 11.5	4 51.0	+28.9	S86 50W	61 39	P.
190			13 23	5 0	+45	N57 24W	64 43	V.
191		Osaka	19 13 17	5 14	+47	N50 21W	66 28	V.
192		Shizuoka	19 14 46	19 16	+76	N 0 7W	20 58	V.
193	Mar. 20, '58	Miyazaki	5 3 57.5	9 8	+56	N32 23W	14 59	V.?
194			5 31	11 0	+57.3	N38 2W	29 11	V.
195			5 57.8	11 46.4	+55.4	N41 37W	35 5	V.
196			6 14.8	12 15	+54.4	N43 16W	39 4	P.
197			6 22.3	12 30	+53.4	N44 38W	41 14	P.
198			6 47.5	13 20	+48.9	N50 26W	49 13	P.?
199			7 11	14 7	+42.7	N59 17W	57 59	P.?
200			7 22	14 21	+39.6	N64 52W	60 53	P.

Table 2. (continued)

No.	Date	Team	Time	R.A.	Declination	Azimuth	Altitude	Remarks
			h m s	h m				
201	Mar. 20, '58	Miyazaki	5 7 25.4	14 26	+38.°5	N67°1′ W	61°54′	P.
202			7 36	14 45	+33.9	N77 27W	65 42	P.
203			7 39.7	14 51	+32.5	N81 11W	66 50	P.
204			7 49	15 4	+28.9	S88 6W	68 55	P.?
205			8 19.6	15 43.9	+15.6	S42 5W	69 4	V.
206			8 57.4	16 22	+ 0.1	S 9 28W	57 49	P.?
207			9 10.2	16 32.5	− 4.4	S 4 7W	53 36	P.
208			9 13.5	16 35	− 5.7	S 3 0W	52 20	P.
209			9 26.4	16 46	− 9.9	S 1 16E	48 10	P.?
210			9 29.5	16 46.6	−10.7	S 1 26E	47 22	V.
211			9 52.6	17 3	−17.1	S 6 18E	40 45	P.?
212			10 4	17 9	−19.5	S 7 45E	38 13	P.
213			10 8	17 12	−20.3	S 8 29E	37 20	P.
214			10 51.1	17 32.5	−27.7	S12 19E	29 16	P.?
215		Kochi	5 7 36	14 11	+19	S77 38W	51 59	V.
216		Kanaya	18 49 5	5 35	− 9	S22 38W	44 17	V.
217			50 15	11 0	+65	N30 28E	41 4	V.
218		Kashiwara	18 49 14	5 22	−12	S25 50W	39 45	V.
219			49 26	5 44	+ 7	S29 24W	59 23	V.
220			50 25	11 5	+67.83	N26 58E	40 51	V.
221			50 52	13 18	+64.5	N28 42E	27 30	V.
222		Osaka	18 49 38	6 35	+16	S 4 46W	71 15	V.
223		Shizuoka	18 49 53	3 45	+23.7	S87 35W	47 53	V.
224			50 49	0	+88.7	N 1 32W	34 40	V.
225		Kwasan	18 49 54.3	7 10.6	+33.4	S76 27E	84 2	P.

Table 2. (continued)

No.	Date	Team	Time	R.A.	Declination	Azimuth	Altitude	Remarks
			h m s	h m				
226	Mar. 20, '58	Kwasan	18 49 56.3	7 17.7	+36.°05	N79 3'E	82°50'	P.
227			50 16.2	9 17.64	+57.66	N36 26E	55 47	P.
228			50 24.1	10 14.68	+62.32	N33 16E	47 32	P.
229			50 38.5	11 49	+64.22	N31 55E	36 54	P.
230			50 42.3	12 13.02	+63.9	N31 51E	34 16	P.
231			50 49.0	12 43.12	+63.71	N31 6E	31 1	P.
232		Yokkaichi	18 50 0	5 59	+46	N35 33W	75 50	V.
233			50 58	12 32	+71	N23 5E	34 4	V.
234	Mar. 21, '58	Kanaya	4 43 24	13 55	+19	S77 32W	51 20	V.
235			45 33	16 1	−21	S10 26W	34 15	V.

P.: photographic V.: visual
*: *no field star because of cloudy* §: *no trail because of sky fog*
&: observed at Kobe ?: reported as uncertain.

The position is given by the right ascension (R.A.) and by the declination of the satellite referred to field stars. The Skalnate Pleso Atlas was used for reference. The Moon Watch teams reported also the observational time and the position at which a good observation was carried out. Table 1 gives the data for the observing teams; the first column gives the current number, the second the place of the observing team, the third the longitude, the fourth the latitude, and the fifth the altitude. The observational data are compiled in Table 2; the first column gives the current number, the second the observational date, the third the observing team, the fourth the observation time, the fifth the right ascension, the sixth the declination, the seventh and the eighth the azimuth and the altitude converted from the right ascension and the declination respectively, and the ninth gives remarks. Hereafter time is referred to the Japanese Standard Time.

II. ORBIT

In this part, we shall describe the method of determining the orbital elements of 1957 β and find them by using the observational data obtained in the Western Japanese territories. According to the Russian communication the orbit of 1957 β is nearly circular, and we can observe only a small part of its orbit on any day. With

further allowance for the observational errors, it is difficult and rather disadvantageous to apply straightforwardly the usual orbital theory to the determination of the orbit of 1957 β. Therefore, we have confined ourselves to the favourable opportunities for us to determine the orbital elements and have treated the subject *graphically*.

3. Basic relations

Under the inverse-square law in the central-force field of the Earth's gravitation, the orbit of satellite is given by the well-known equation for an ellipse:

$$r = p(1+\varepsilon\cos v)^{-1}, \quad \text{with} \quad p = a(1-\varepsilon^2), \quad r = R_\phi + H, \tag{1}$$

where r is the radius vector from the Earth's center to the satellite, a the semi-major axis, ε the eccentricity, v the true anomaly, R_ϕ the radius of the Earth at the latitude ϕ, and H is the height of the satellite above the sea level. r/a is illustrated in Fig. 3, taking ε as a parameter.

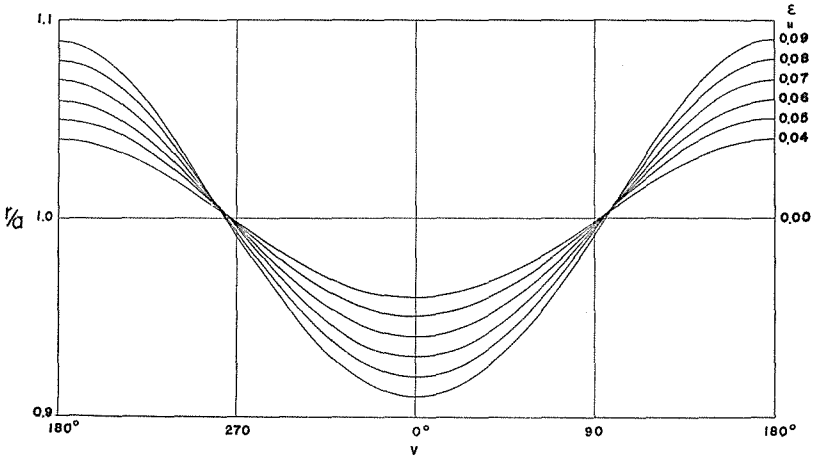

Fig. 3. The behavior of r/v *versus* v, taking ε as a parameter.

It is useful also to give the Keplerian expressions for the period T and for the orbital velocity V of an elliptical orbit;

$$\left.\begin{aligned} T &= 2\pi(GM)^{-1/2}a^{3/2}, \\ V &= (GM)^{1/2}\left(\frac{2}{r}-\frac{1}{a}\right)^{1/2}, \end{aligned}\right\} \tag{2}$$

where G is the gravitational constant and M is the mass of the Earth. R_ϕ decreases by several kilometers from 30°N to 40°N. In Fig. 4 are shown the relations (2), taking H above the 35°N sea level as a parameter.

Let h be the observed altitude of the satellite and θ the angle with which the

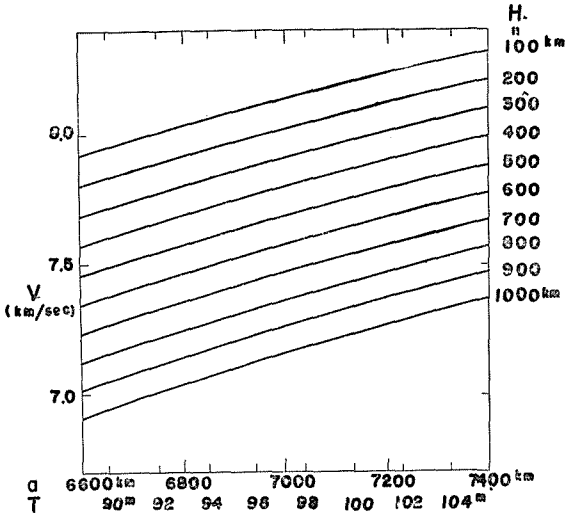

Fig. 4. The behavior of V *versus* a or T, taking H above the 35°N sea level as a parameter.

observer and the satellite subtend at the Earth's center. Then h is safely connected with θ and H by the relation:

$$\tan h = \cot\theta - \frac{R_\phi}{r}\operatorname{cosec}\theta\,, \quad (3)$$

in which it is assumed that the altitude of the observatory is not too high and that the latitude of the observed point of the satellite is not too different from that of the observatory. The relation (3) is illustrated in Fig. 5, taking H above the 35°N sea level as a parameter.

Lastly it is convenient to

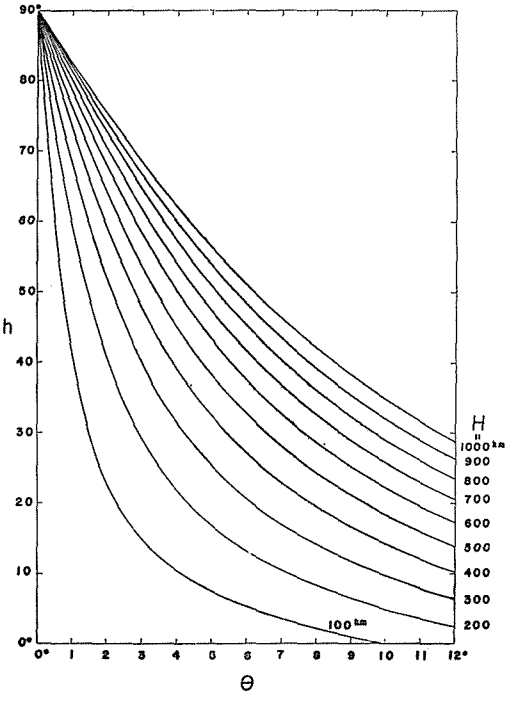

Fig. 5. The behavior of h *versus* θ, taking H above the 35°N sea level as a parameter.

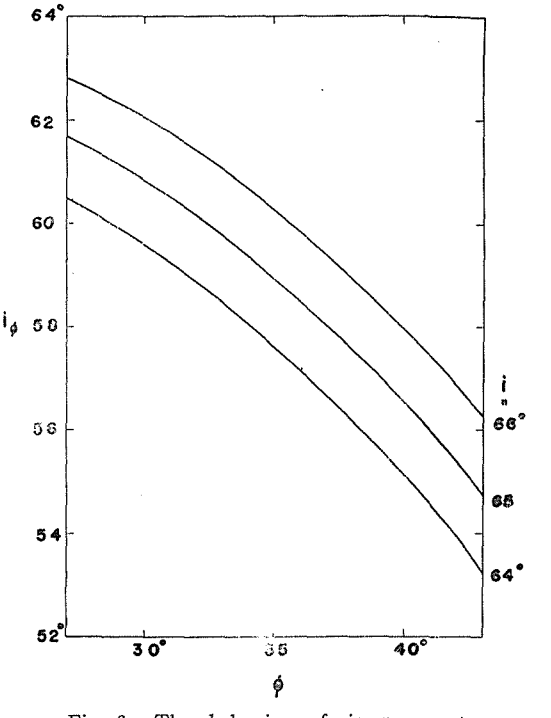

Fig. 6. The behavior of i_ϕ *versus* ϕ, taking i as a parameter.

have the inclination i_ϕ of the orbit projected on the surface of the Earth to any latitude line. Let i be the inclination of the orbit to the equatorial plane, then i_ϕ is given by

$$\cos i_\phi = \cos i \sec \phi\,, \quad |\phi| \leqslant i\,. \tag{4}$$

The relation (4) is shown in Fig. 6, taking i as a parameter. Corresponding to $i=64°$, 65° and 66°, we have prepared three curved measures drawn on a transparent celluloid sheet so as to fit the scale of the chart (1).

4. Determination of height

As is seen from the relation (3), the observed altitude is a function of θ and H. In other words, we cannot plot the observational data on the chart without knowing H. Moreover, (1) and (2) show that H is a fundamental quantity which determines the orbital elements. Then we shall take a glance at methods of fixing H.

a) It is obvious that the trigonometric survey is the most useful and precise method of determining H.

b) The orbital velocity of the satellite is connected with H by the relation (2). We may find out H from pass length of the satellite orbit projected on the chart, taking H as a parameter. H is, of course, variable when the time interval of the observations is too long, whereas change of the pass length due to that of H is negligible for $\Delta v \lesssim 5°$ for 1957 β with $\varepsilon \lesssim 0.1$. Namely, the pass length on the chart is approximated by R_ϕ/r times that in space. It is to be noted, however, that this method of determining H is such as to estimate the mean height over the time interval of observations.

c) We may employ a new trial of determining H from the observations at only *one* place in the absence of trigonometric survey. By means of the one place observations of the successive crossings of the east-west line for three days, we can simultaneously fix the mean height for three days at that latitude and $\Delta\Omega$, the retrograde rate of orbit per day. Let t_i and λ_i be the time and the longitude of the crossing of the east-west line for the i-th day, respectively. Then t_i and λ_i are connected with those in the following day by the relation:

$$\lambda_{i+1}-\lambda_i = (t_i-t_{i+1}) - \left(1-\frac{t_i-t_{i+1}}{\text{one day}}\right)(\Delta\Omega+\Delta\Phi)\,, \tag{5}$$

where $\Delta\Phi$ is the rate of revolution of the Earth around the Sun per day and is put nearly as 0.°986. Using the relation (5) we derive for λ_2 and λ_3

$$\left.\begin{aligned} \lambda_2 &= \lambda_1 - \left(1-\frac{t_1-t_2}{1440}\right)\Delta\Omega + \frac{1}{4}(t_1-t_2) - \left(1-\frac{t_1-t_2}{1440}\right)\Delta\Phi\,, \\ \lambda_3 &= \lambda_1 - \left(2-\frac{t_1-t_3}{1440}\right)\Delta\Omega + \frac{1}{4}(t_1-t_3) - \left(2-\frac{t_1-t_3}{1440}\right)\Delta\Phi\,, \end{aligned}\right\} \tag{6}$$

where t_i-t_j is expressed in minutes of time, each term in degrees of arc, and $\Delta\Omega$ is assumed not to change during those days.

Now, we shall apply the relations (6) to the evening observations on March 18, 19 and 20 in 1958. Of course, the crossing longitudes λ_i's depend apparently on H. Using each observational time and λ_1 which depends on H, we shall compute λ_i $(i=2, 3)$ from (6) taking $\Delta\Omega$ as a parameter, and shall plot λ_i in Fig. 7. On the other hand, we know λ_i $(i=2, 3)$ from the observations as the function of H, and plot λ_i in Fig. 7. Then, we can uniquely fix $H=255$ km and $\Delta\Omega=3.°18$, assuming that H has not changed during three days. The observation on March 18 was considerably apart from our east-west line, and so we are obliged to extrapolate its data to this line (see §5). Hence the values of H and $\Delta\Omega$ fixed above might be somewhat incorrect.

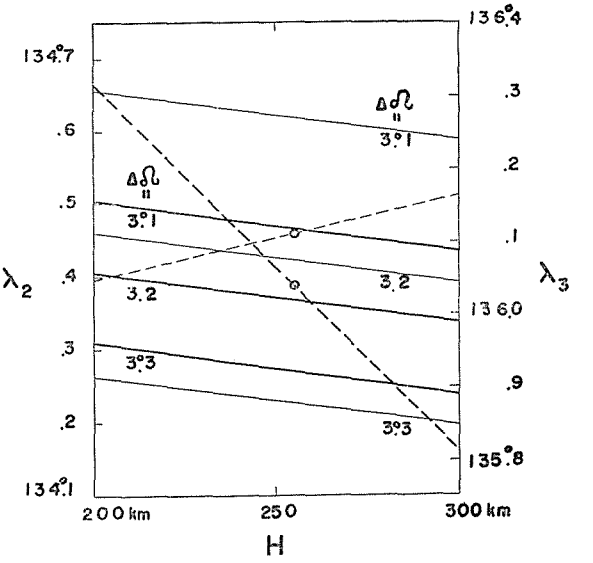

Fig. 7. The computed behaviors of λ_2 and λ_3 *versus* H taking $\Delta\Omega$ as a parameter are expressed by the solid curves, and the observed ones for λ_2 and λ_3 *versus* H by the dashed. λ_2 in thick curve is read by the left-hand ordinate scale, and λ_3 in thin by the right-hand one.

The change of H per day might be of the order of several kilometers and that of $\Delta\Omega$ per day of the order of a few thousandths of degree for 1957 β. Therefore, in treating the subject, the said assumptions may be admissible particularly for the observations in the perigee regions, with allowance for the observational errors. If we are able to have successive observations day by day, we may find the daily changes for H and $\Delta\Omega$. The present method is, however, not so effective with the exception of such a case that the observing place lies between the successive crossings.

5. Period and retrograde rate of orbit

If we can observe the times of the successive crossings of the east-west line of the observing place, we can find the period in which the satellite revolves around the Earth. It is, however, of rare occurrence to observe the successive passages within a day. Moreover, we have not always the east-west line observations. Therefore it

is necessary to extrapolate the observed points to one latitude line. We shall fix that line to the 35°N one passing near Kwasan Observatory. After finding H by means of such methods in the preceding section, we can plot the observed points on the chart using the data given in Table 2. When the observed point is apart from the 35°N line, it is extrapolated to that line along the curved measure mentioned in § 3. The observed point for the extrapolation should be such as more close to the 35°N line and more precise in observations. Until the inclination i is determined, it is assumed as 65° according to the Russian announcement. Then, we can find the time and the longitude at which the satellite crosses the 35°N line. Of course, the rotation of the Earth for the time interval between the two successive observations must be taken into account. From the successive crossings for two days, the mean period over about one day, T_ϕ, may be obtained in general by the following relation:

$$1440 = NT_\phi + \tau\,, \quad T_\phi > \tau\,, \tag{7}$$

where τ is the time in minutes by which N revolutions fall short of one day. $\Delta\Omega$, the retrograde rate of orbit per day, is directly obtained from the relation (5).

In Table 3 are listed the several quantities reduced as above with exception of those obtained from observations unfavourable for reductions. The first column in Table 3 gives the date of observation, the second the mean height for the two or three days, the third the crossing time, the fourth the crossing longitude, each on the 35°N line, the fifth the date on which the mean period is fixed, the sixth the mean period over about one day, and the seventh the retrograde rate of orbit per day. The explanation as to the figure in the bracket in the sixth column will be postponed to § 9. The errors estimated are such as incurred through the uncertainty of H and partly through those of the observation time, the inclination, the operations of plotting the observational data and of extrapolating to the 35°N line, and so on.

6. Eccentricity

The orbit of 1957 β is nearly circular and we can observe only a small part of its orbit within one day. Practically we had not so precise observation of heights as to determine the orbital elements, only by the Western Japanese territory observations for one day. However, it we have successive observations evening after morning or morning after evening, we can determine the eccentricity of the orbit, provided that the orbital elements do not change for those intervals. For we can observe considerably separate parts of the orbit on the morning and on the evening. We had such a case on March observations.

Now we shall determine the eccentricity on March 20.000 by using the observational data on March 19 evening and on March 20 morning. Let the quantities of

Table 3.

Date	35° N			Date	T_ϕ (T)	$\Delta\Omega$
	H	t	λ			
Nov. 6, '57		h m 5 10.841 m ±0.100	138.°97 ±0.°04			
	295 km ±20 km			Nov. 6.720	m 103.610 m ±0.009 m (103.600)	2.°19 ±0.°26
Nov. 7, '57		5 21.383 ±0.020	133. 13 ±0. 19			
Dec. 15, '57		5 39.357 ±0.010	132. 06 ±0. 09			
				Dec. 15.730	101.688 ±0.003 (101.679)	2. 68 ±0. 19
Dec. 16, '57	870 ±20	5 22.992 ±0.025	132. 53 ±0. 09			
				Dec. 16.718	101.635 ±0.004 (101.626)	2. 68 ±0. 18
Dec. 17, '57		5 5.879 ±0.030	133. 19 ±0. 08			
Dec. 23, '57		17 53.181 ±0.012	134. 20 ±0. 12			
	212 ± 5			Dec. 24.237	101.232 ±0.002 (101.223)	2. 57 ±0. 16
Dec. 24, '57		17 30.433 ±0.013	136. 38 ±0. 03			

Table 3. (continued)

Date	35° N			Date	T_ϕ (T)	$\Delta\Omega$
	H	t	λ			
Jan. 23, '58		h m 19 21.233 m ±0.020	136.°21 ±0.°05			
				Jan. 24.288	m 99.144 m ±0.002 m (99.135)	2.°79 ±0.°26
Jan. 24, '58	895 km ±20 km	18 29.245 ±0.010	145. 57 ±0. 20			
				Jan. 25.286	99.063 ±0.002 (99.054)	2. 84 ±0. 33
Jan. 25, '58		19 15.185 ±0.010	130. 13 ±0. 13			
Mar. 18, '58		19 34.673 ±0.017	133. 13 ±0. 03			
				Mar. 19.308	94.569 ±0.002 (94.561)	3. 18 ±0. 08
Mar. 19, '58	254 ±5	19 13.212 ±0.010	134. 39 ±0. 05			
				Mar. 20.293	94.447 ±0.001 (94.439)	3. 19 ±0. 08
Mar. 20, '58		18 49.922 ±0.010	136. 11 ±0. 03			
Mar. 19, '58		5 29.010 ±0.039	125. 73 ±0. 10			
				Mar. 19.721	94.520 ±0.004 (94.512)	
Mar. 20, '58	715 ±20	5 6.812 ±0.017	127. 01 ±0. 08			
				Mar. 20.705	94.399 ±0.003 (94.391)	
Mar. 21, '58		4 42.790 ±0.021	128. 83 ±0. 16			

the former be denoted by suffix e and those of the latter by suffix m. From the data in Table 3 we may find for the difference of the true anomalies $v_m - v_e$ between the 19 evening and the 20 morning, in an approximation of no motion of the perigee along the orbit:

$$\left.\begin{aligned} \cos(v_m - v_e) &= 1 - \cos^2 35° + \cos^2 35° \cos \Theta , \\ \text{then} \qquad & \\ v_m - v_e &= 101.°83 , \end{aligned}\right\} \tag{8}$$

where

$$\Theta = \left(1 - \frac{t_e - t_m}{\text{one day}}\right)(360° + \Delta\Omega + \Delta\Phi) - (\lambda_e - \lambda_m) = 142.°74 ,$$

with

$$\Delta\Omega = 3.°18 .$$

On the other hand, we have $a = 6871$ km from the mean period $T \simeq T_\phi = 94.^m485$ (see § 9), and have $r_e = 6625\,\text{km} \pm 5\,\text{km}$ and $r_m = 7086\,\text{km} \pm 20\,\text{km}$ corresponding to $H_e = 254\,\text{km} \pm 5\,\text{km}$ and $H_m = 715\,\text{km} \pm 20\,\text{km}$ respectively. Then we have

$$\left.\begin{aligned} r_e/a &= 0.9642 \pm 0.007 , \\ r_m/a &= 1.0313 \pm 0.029 . \end{aligned}\right\} \tag{9}$$

By applying (8) and (9) to Fig. 3, we find out graphically, for the mean eccentricity ε and also for v_e:

$$\varepsilon \text{ (Mar. 20.000)} = 0.043 \pm 0.0020 , \tag{10}$$

and

$$v_e \text{ (Mar. 20.000)} = 35.° \pm 4.°0 . \tag{11}$$

The latitude of the perigee on those days may be found about 3°N with the value (11) and that of the apogee about 3°S, by assuming the inclination i as 65°. Then, we can obtain, by (10), for the heights of the perigee and the apogee:

$$\left.\begin{aligned} H_P \text{ (Mar. 20.000)} &= 195\,\text{km} \pm 14\,\text{km} , \\ H_A \text{ (Mar. 20.000)} &= 791\,\text{km} \pm 14\,\text{km} , \end{aligned}\right\} \tag{12}$$

where the suffixes P and A are referred to the perigee and the apogee, respectively.

7. Inclination

From the analysis in the preceding section we have found the dimensions and the direction of the orbit with respect to the Earth from March 19 to 20. Therefore we can compute the heights of 1957 β at every latitude of the Earth, assuming at first that the inclination i is equal to 65°. In fact, the heights computed above are seen hardly dependent on i as long as the uncertainty for i is of the order of $\pm 1°$. We shall apply these heights to the photographic and comparatively precise observations

on March 20 morning obtained by Miyazaki Team and find the height for every observation, which is listed in Table 4. The 1st column of Table 4 gives the current number in Table 2, the 2nd the latitude of the observed point which is estimated from the azimuth and from the first approximation height, and the 3rd the height computed corresponding to the 2nd column latitude. Using the heights ih Table 4 we can plot the observational data on the chart, of course, with allowance for the rotation of the earth corresponding to the observation times. This determines the orbit projected on the earth's surface. By making the curved measures quoted in §3 slide on this orbit we may find for the inclination

Table 4.

No.	ϕ	H
196	36.°7N	707 km
197	36. 3	709
200	33. 3	721
201	33. 1	722
202	32. 5	724
203	32. 3	725
305	30. 2	732
207	27. 6	741
208	27. 4	742

$$i = 65.^\circ5 \pm 0.^\circ2 . \tag{13}$$

Without all these valuable data which were put at our disposal by Miyazaki Team, it would have been impossible to make this determination.

8. Motion of the perigee along the orbit

It is known by the perturbation theory that the perigee is in motion along the orbit corresponding to the retrograde motion of the orbit. We shall seek for the rate of the perigee motion.

It is probable that the change of the perigee height with time is very slow compared to that of the apogee one, so we can say from the values in Table 3 and in (12) that we had the observation near the perigee regions on December 23 evening. Therefore, it may be permissible to extrapolate the height on December 23 to that on December 16. Namely, on December 16, 1957 β might have crossed with $H_e \simeq 232$ km or more* near evening while with $H_m = 870$ km $\pm$ 20 km on the morning. As we have, however, no informations on the time and the longitude of the evening crossing, we cannot evaluate $v_m - v_e$. Assuming a circular orbit with $i = 65.^\circ5$ we shall estimate $v_m - v_e$ nearly as 102°. Then, following the procedure as in §6 we may find for ε and v_e:

$$\varepsilon \ (\sim \text{Dec. } 16) \simeq 0.088 , \tag{14}$$

and

$$v_e \ (\sim \text{Dec. } 16) \simeq 354^\circ \ (= -6^\circ) . \tag{15}$$

The latitude of the perigee may be found with (15) near 40°N and that of the apogee

* This will be justified in a later analysis.

near 40°S. Then we get, by (14), the heights of the perigee and the apogee as:

$$\left.\begin{aligned} H_P \ (\sim\text{Dec. } 16) &\simeq 210\,\text{km}\,, \\ H_A \ (\sim\text{Dec. } 16) &\simeq 1480\,\text{km}\,. \end{aligned}\right\} \tag{16}$$

In the first approximation of its linear motion, we may find, for the motion of the perigee along the orbit per day from Debember 16 to March 20,

$$\Delta\omega \simeq \frac{-6-35.8}{94} = -0.44 \text{ degrees per day}. \tag{17}$$

That is, the perigee might retrograde along the orbit at the mean rate of 0.44 degrees per day. When we extrapolate, with (17), linearly back to the launching days, we may guess that the latitude of the perigee for those days was near 55°N.

As will be shown later, the period and the retrograde motion of the orbit do not change linearly with respect to time. The retrograde motion of the orbit seems further to be in some relation to the period. The perigee motion is connected with the retrograde motion of the orbit, so the former must, in fact, have a dependency like that of the latter on the period.

Up to the preceding section we have neglected the perigee motion in describing the orbit. In the next section we shall briefly consider an influence of the present motion on the period and shall give the period in its true sense.

III. RESULTS

We shall derive some results from the orbital elements and their changes of 1957 β obtained in the preceding part.

9. Period in the true sense and its acceleration rate

Owing to the perigee motion along the orbit, the period in the true sense T is expected to be different from T_ϕ, the period between the successive crossings of 35°N line. T may be connected with T_ϕ by the relation:

$$T = T_\phi\left(1+\frac{\Delta\omega\, T_\phi}{360\times 1440}\right). \tag{18}$$

With (17), as for 1957 β, it is found that T is shorter by about $0.^{m}01$ than T_ϕ in the first appro ximation. The period in the true sense is bracketed in the sixth column of Table 3.

As a result of the transformation of T_ϕ into T, the semi-major axis introduced in §§ 6 and 8 should be made smaller by about 0.5 km and, consequently, the results in sections from 6 to 8 must suffer some changes. However these are included within the errors, so we shall leave the results as they were.

Next we shall estimate the acceleration rate of the period. The mean rate per day may be approximated by a rough formula:

$$\Delta T = \frac{\delta T}{\delta t}, \tag{19}$$

where δt means the difference of time in days on which T's are fixed, and δT the increment of the period for that interval. The data made use of for determining ΔT are listed in Table 5 with reference to Table 3. The first column of Table 5 gives the date on which T is fixed, the second the period, the third δT, the fourth δt, the fifth the mean date on which ΔT is determined, and the sixth the acceleration rate of the period per day obtained from (19).

Table 5.

Date	T	δT	δt	Date	ΔT
	m	m	d		m
Nov. 6.720	103.600	−1.830	37.032	Nov. 25.236	−0.0494
Dec. 13.752	101.770*	−0.144	2.966	Dec. 15.235	−0.0485
Dec. 16.718	101.626	−0.403	7.519	Dec. 20.478	−0.0536
Dec. 24.237	101.223	−2.088	31.051	Jan. 8.762	−0.0672
Jan. 24.288	99.135	−0.385	5.978	Jan. 27.313	−0.0644
Jan. 30.266	98.750*	−3.908	45.430	Feb. 21.981	−0.0860
Mar. 16.696	94.842*	−0.451	4.009	Mar. 18.701	−0.1124
Mar. 20.705	94.391				

* Less certain data which are not listed in Table 3.

The behaviors of T and ΔT with respect to date are illustrated in Fig. 8 with reference to Table 3 and to Table 5. The behavior of ΔT is very curious. The discussions on this erratic orbital acceleration were given partly by L. G. Jacchia (**2**). We shall, however, have no comment on this interesting subject only from our observations.

10. Dependency of the retrograde rate of orbit on the period

The retrograde motion of the orbit is due to the non-central field of terrestrial gravitation, so the retrograde rate is expected to depend on the mean height of the satellite. From Table 3 it is found that the retrograde per day tends to increase in fact with the period decreasing We shall now seek for an empirical formula between $\Delta\Omega$, the retrograde rate of the orbit per day, and the period in the true sense T.

In treating the subject we shall make use of a mean value of the retrograde motion, for its daily rate tabulated is considerably incorrect due to the uncertainty of the

crossing longitude. We shall define for its mean value from the i-th day to the $(i+n)$-th day which belongs to the next observation series and corresponds to the cycle with the same true anomaly, apart form the perigee motion

$$\overline{\Delta\Omega} = \frac{1}{\delta t'}\{(\lambda_i - \lambda_{i+n}) + (t_i - t_{i+n})\} - \Delta\Phi\,, \tag{20}$$

with

$$\delta t' = (n-1) - \frac{t_i - t_{i+n}}{\text{one day}}\,, \tag{20}$$

where $t_i - t_{i+n}$ in the right-hand side of (20) is always to be positive, making allowance for the retrograde rate of the oribit from the i-th day to the $(i+n)$-th day. The data for determining $\overline{\Delta\Omega}$ and the dependency of $\Delta\Omega$ on T are compiled in Table 6 with reference to Table 3. The data in the first, the second and the third columns of Table 6 are those in Table 3, while the fourth gives the difference of time in days between the neighbouring dates, the fifth the mean rate of the retrograde motion per day obtained, and the sixth the period for each date in the first column, extrapolated using the data in Table 3. The seventh will be explained later.

Table 6.

Date	t	λ	$\delta t'$	$\overline{\Delta\Omega}$	T	T
	h m		d		m	m
Nov. 7, '57	5 21.383	133.°13	46.522	2.°689	103.577	102.446
Dec. 23, '57	17 53.181	134. 20	87.040	2. 965	101.250	98.079
Mar. 20, '58	18 49.922	136. 11			94.378	
Dec. 16, '57	5 22.992	132. 53	39.546	2. 817	101.652	100.464
Jan. 24, '58	18 29.245	145. 57	54.443	3. 040	99.093	96.998
Mar. 20, '58	5 6.812	127. 01			94.451	
*Mar. 19.9, '58				3. 18		94.486

* Direct observational datum on March 18, 19 and 20 evenings in 1958.

Now we shall empirically set forth the relation between $\Delta\Omega$ and T in the form:

$$\Delta\Omega = KT^k\,, \tag{21}$$

where K and k are constants. The mean rate of the retrograde motion with respect to the period from the i-th day to the $(i+n)$-th day is

$$\frac{1}{T_{i+n} - T_i}\int_{T_i}^{T_{i+n}} \Delta\Omega dT = \frac{K}{k+1}\left(T_{i+n}^{k+1} - T_i^{k+1}\right)\,. \tag{22}$$

As is seen from Fig. 8 the period does not vary linearly with respect to time, so the mean value (20) is not strictly equal to the mean value (22). As a rough approximation, however, we shall seek for the constants K and k by equating (20) to (22).

The empirical formula between $\Delta\Omega$ and T thus obtained by using the data for four intervals in Table 6 may be given as follows:

$$\Delta\Omega = (4.49 \pm 0.01) \times 10^4 T^{-2.1 \pm 0.1}, \tag{23}$$

where $\Delta\Omega$ is in degrees of arc, and T in minutes of time. Further $\Delta\Omega$ is known linearly dependent on $\cos i$, so we get with (13) and (23)

$$\Delta\Omega = (1.08 \pm 0.01) \times 10^5 \cos i \; T^{-2.1 \pm 0.1}. \tag{24}$$

Fig. 8 shows that the period considerably deviates from the linearity with respect to time for such intervals as given in Table 6. The longer the intervals, the errors of $\overline{\Delta\Omega}$ incurred through the uncertainties of longitudes are smaller, whereas the permissibility of equating (20) to (22) is broken. Then we shall take $\overline{T}$, the mean period

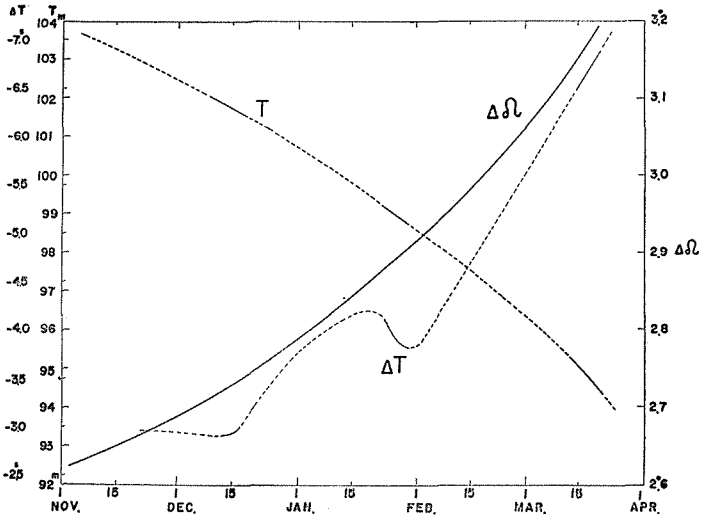

Fig. 8. The behaviors of T and ΔT *versus* date: T in minutes of time, ΔT in seconds of time; the solid curve is such as obtained directly from the observations, the dashed curve as intercombined smoothly. The behavior of $\Delta\Omega$ *versus* T or date (see § 10).

with respect to long time, approximating T by the quadratic curve with respect to time from the i-th day to the $(i+n)$-th day. $\overline{T}$ thus obtained is given in the seventh column of Table 6. As an alternative approximate method for finding out the relation (21), we shall make $\overline{\Delta\Omega}$ correspond, one to one, to $\overline{T}$ for each interval. By means of the method of least squares with five data in Table 6 we derive other formulae:

$$\Delta\Omega = 4.36 \times 10^4 T^{-2.093} \pm 0.01, \tag{25}$$

and

$$\Delta\Omega = (1.05 \pm 0.01) \times 10^5 \cos i \; T^{-2.093} \pm 0.01. \tag{26}$$

Numerically the value (25) is larger than (23) by about 0.°01 throughout the period of 1957 β. The empirical formulae (23) and (24) are illustrated respectively in Figs. 8 and 9, by taking the inclination i as a parameter.

Since the air resistance to the satellite may be expected to have the same component of force as that due to non-central terrestrial gravitation in accordance with the shape and with the flying mode of the satellite the relation (24) or (26) is not universal.

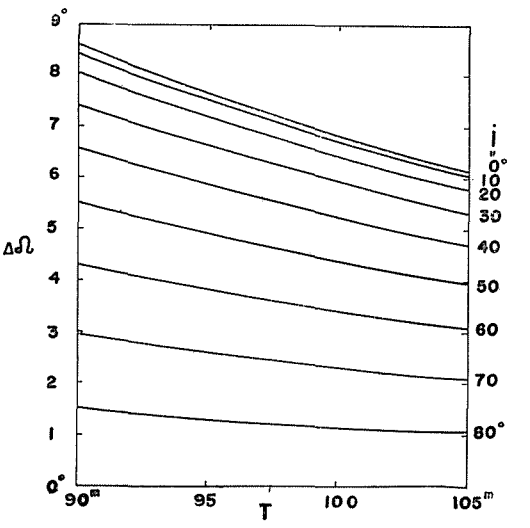

Fig. 9. The behavior of $\Delta\Omega$ *versus* T, taking i as a parameter.

11. Atmospheric density

The work performed by air resistance to the satellitc diminishes its total energy, and the dimensions of the orbit progressively decrease. In other words, we may be able to determine the atmospheric density by observing the changes of the orbital elements.

We shall treat the subject following the analysis given by I. M. Yaçunski (3). He confines himself to the plane orbit problem. Namely, no perturbations of the node or of the inclination occur. Likewise he takes no account of the secular perturbations of perigee. Therefore his treatment reduces to calculating merely the secular perturbations of the parameter p and thd eccentricity ε of the orbit.

For the acceleration Γ due to air resistance we may have

$$\Gamma = \frac{C\sigma_s}{2m_s}\rho V^2 = \frac{1}{2}b\rho V^2, \tag{27}$$

with

$$b = \frac{C\sigma_s}{m_s}, \tag{28}$$

where ρ is the air density, C the coefficient of air resistance, V the orbital velocity, σ_s the frontal cross-sectional area and m_s the mass of the satellite.

On the basis of the plane orbit problem, we shall have the differential equations for determining p and ε as functions of v as:

$$\frac{dp}{dv} = \frac{r^2}{GM}\cdot 2rY, \tag{29}$$

and

$$\frac{d\varepsilon}{dv}=\frac{r^2}{GM}\left\{X\sin v+\left(1+\frac{r}{p}\right)Y\cos v+\varepsilon\frac{r}{p}Y\right\}, \tag{30}$$

where X and Y are the projections of the perturbing acceleration on the radius vector and on the perpendicular to the radius vector in the plane of the ellipse, respectively. X and Y may be given by

$$\left.\begin{aligned}X&=-\frac{\Gamma}{V}\left(\frac{GM}{p}\right)^{1/2}\varepsilon\sin v=-\frac{1}{2}b\rho\frac{GM}{p}\varepsilon\sin v(1+2\varepsilon\cos v+\varepsilon^2)^{1/2},\\ Y&=-\frac{\Gamma}{V}\left(\frac{GM}{p}\right)^{1/2}(1+\varepsilon\cos v)=-\frac{1}{2}b\rho\frac{GM}{p}(1+\varepsilon\cos v)(1+2\varepsilon\cos v+\varepsilon^2)^{1/2}.\end{aligned}\right\} \tag{31}$$

Substituting the expressions (31) into (29) and (30), we get

$$\frac{dp}{dv}=-b\rho p^2(1+2\varepsilon\cos v+\varepsilon^2)^{1/2}(1+\varepsilon\cos v)^{-2}, \tag{32}$$

and

$$\frac{d\varepsilon}{dv}=-b\rho p(\varepsilon+\cos v)(1+2\varepsilon\cos v+\varepsilon^2)^{1/2}(1+\varepsilon\cos v)^{-2}. \tag{33}$$

For the density distribution, we shall assume the exponential function of the type

$$\rho=Ae^{-\alpha H}, \tag{34}$$

where A and α are constants. Substituting (34) into (32) and (33) with the relations (1) and expanding these into power series and retaining terms of order ε^2 with allowance for the smallness of ε, we get, instead of (32) and (33),

$$\begin{aligned}\frac{dp}{dv}=Abp^2e^{-\alpha(p-R_\Phi)}e^{x\cos v}&\left(1-\varepsilon x\cos^2 v+\frac{\varepsilon^2}{2}x^2\cos^4 v\right)\\ &\times\left\{\left(1+\frac{\varepsilon^2}{2}\right)-\varepsilon\cos v+\frac{\varepsilon^2}{2}\cos^2 v\right\},\end{aligned} \tag{35}*$$

and

$$\begin{aligned}\frac{d\varepsilon}{dv}=-Abpe^{-\alpha(p-R_\Phi)}e^{x\cos v}&\left(1-\varepsilon x\cos^2 v+\frac{\varepsilon^2}{2}x^2\cos^4 v\right)\\ &\times\left\{\varepsilon+\left(1-\frac{\varepsilon^2}{2}\right)\cos v-\varepsilon\cos^2 v+\frac{\varepsilon^2}{2}\cos^3 v\right\},\end{aligned} \tag{36}$$

with

$$x=\alpha p\varepsilon. \tag{37}$$

Let η denote the number of revolutions around the Earth. We shall integrate (35) and (36) with respect to v between the limits 0 and $2\pi\eta$, assuming that the changes of p and ε are negligibly small in this interval. Then we have approximately

$$p-p_0=-2\pi\eta Abp_0^2e^{-\alpha(p_0-R_\Phi)}F_p(x), \tag{38}$$

and

$$\varepsilon-\varepsilon_0=-2\pi\eta Abp_0e^{-\alpha(p_0-R_\Phi)}F_\varepsilon(x), \tag{39}$$

* Hereafter, we have somewhat different expressions from those given by YAÇUNSKI (3).

with

$$F_p(x) = \left\{(1+\varepsilon_0^2) - \varepsilon_0 x + \frac{\varepsilon_0^2}{2}x^2\right\} I_0(x) - \frac{\varepsilon_0^2}{2x} I_1(x) + \frac{\varepsilon_0^2}{2} I_2(x), \tag{40}$$

and

$$F_\varepsilon(x) = \left\{\frac{\varepsilon_0}{x} + (1-\varepsilon_0^2) - \varepsilon_0 x + \frac{\varepsilon_0^2}{2}x^2\right\} I_1(x) + \\ + \left(\frac{5\varepsilon_0^2}{2x} + \varepsilon_0 - \varepsilon_0^2 x\right) I_2(x) + \frac{3\varepsilon_0^2}{2} I_3(x), \tag{41}$$

where $I_i(x)$'s $(i=0, 1, 2, 3)$ are modified Bessel functions and the suffix zero denotes the initial values. Eliminating A from (38) and (39) we get

$$\frac{p-p_0}{p_0} \Big/ (\varepsilon - \varepsilon_0) = \frac{F_p(x)}{F_\varepsilon(x)}. \tag{42}$$

Now we shall find out the constant α for those days in March observations. As the starting data March 19.308 will be taken, and as the ending March 20.705. We shall assume, in the first approximation, that the increment of eccentricity for short time interval may be equal to $\frac{2}{3}\frac{\delta T}{T_0}$. Then, from the data in Table 3 and from the value given in (10) we have

$$\left.\begin{aligned} \varepsilon_0 &= 0.0440, \quad p_0 = 6862\,\text{km}, \quad \text{for Mar. } 10.308, \\ \varepsilon &= 0.0428, \quad p = 6854\,\text{km}, \quad \text{for Mar. } 20.705. \end{aligned}\right\} \tag{43}$$

Using the values (43) we evaluate the right-hand side of (42) for the probable range of x. This is given in Table 7. The second column of Table 7 is the scale height calculated from (37) and (43), for x in the first column. As is seen from Table 7, $F_p(x)/F_\varepsilon(x)$ decreases very slowly with increasing x and is close to unity for a considerable range of x. On the other hand, the value of the left-hand side of (42) is nearly equal to unity in the first approximation. Consequently we cannot uniquely fix x unless there are very precise and successive observational data for the parameter p and the eccentricity ε.

Table 7.

x	$1/\alpha$	$F_p(x)/F_\varepsilon(x)$
1	293 km	2.125
2	147	1.378
3	98	1.189
4	73	1.115
5	59	1.078
6	49	1.056
7	42	1.041
8	37	1.031
9	33	1.024
10	29	1.018

In order to limit x to a narrower range the following procedure may be taken, though this is not substantially different from the above. The left-hand side of (42) is analytically given, retaining terms of order ε, by

$$\frac{p-p_0}{p_0} \Big/ (\varepsilon - \varepsilon_0) = 1 + 2\frac{\delta H_P}{\delta H_A} - \varepsilon, \tag{44}$$

where $\delta H_P/\delta H_A$ is the ratio of the increment of the perigee height to that of the

apogee one. We cannot, however, know this reliable value by March observations. From (12) and (16) we may estimate the mean value of $\delta H_P/\delta H_A$ to be about 0.02 from December 16 to March 20. On the other hand, if a supposition that 1957 β burnt out for example in a circular orbit at 150 km altitudes on April 14 is admissible, we may estimate the mean value of $\delta H_P/\delta H_A$ to be about 0.07 from March 20 to April 14. Then we shall roughly assume that $\delta H_P/\delta H_A$ near on March 20 is bounded by

$$0.03 < \frac{\delta H_P}{\delta H_A} < 0.06\,, \tag{45}$$

from which we have for (44)

$$1.017 < \frac{p-p_0}{p_0} \Big/ (\varepsilon - \varepsilon_0) < 1.077. \tag{46}$$

Then, from (42), (46) and Table 7, we get finally for $1/\alpha$

$$29\ \text{km} < \frac{1}{\alpha} < 59\ \text{km}\,. \tag{47}$$

Next we shall return to Eq. (38). b may be estimated as $1.18\times10^{-2}\ \text{m}^2\text{kg}^{-1}$ with $C\simeq 2$, $\sigma_s \simeq 3\ \text{m}^2$ and $m_s = 508.3$ kg. Using (43), $\eta = 21.29$ and $R_\phi = R_{3°\text{N}} = 6378$ km we have for A

$$A = 10^{-10} \times \frac{e^{4.84\times10^2\alpha}}{F_p(x)}\ \text{kg m}^{-3}\,. \tag{48}$$

The restriction (47) and the expression (48) will determine a probable range for the density distribution (34). This is illustrated in Fig. 10.

In short, what we can say about the density distribution at about 195 km altitudes above the equatorial regions is no more than that, corresponding to 30 km<scale height<60 km, the air density lies between $10\times10^{-10}\ \text{kg m}^{-3}$ and $6\times10^{-10}\ \text{kg m}^{-3}$. Further the lack of reliable information on b will make the above values uncertain by factor two.

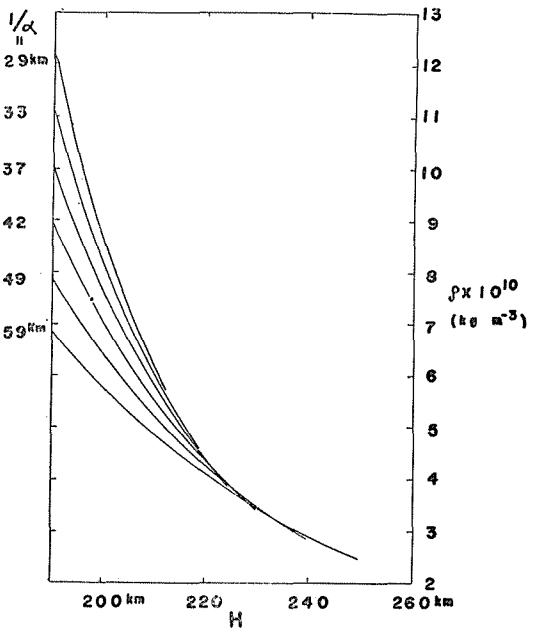

Fig. 10. The behavior of ρ *versus* H, taking $1/\alpha$ as a parameter.

12. Acknowledgement

We wish to express our sincere

thanks to Professor S. Miyamoto, who planned this work and encouraged us throughout the observations.

Our thanks are due to Press the Osaka Yomiuri for financial supports and for communications that made this investigation possible; to Kotobukiya Co., Ltd. under whose sponsorship the Schmidt cameras were constructed; to Osaka Industrial Research Institute (Ikeda Station) for making a 60 cm mirror gratis; and to Fuji Photo Film Co., Ltd. for technical advices and for furnishing photographic materials.

In particular, we are grateful to Western Japanese Moon Watch teams, especially to Miyazaki Team headed by Dr. M. Inaba and also to Kanaya Team headed by Dr. K. Komaki who placed many valuable data at our disposal.

Lastly it is our pleasure to thank Messrs. I. Kawaguchi, S. Tominaga, J. Kubota, T. Inada and others at Kwasan Observatory for their co-works, M. T. Osaki for his helpful discussion, and Dr. J. Jugaku for reading the manuscript.

REFERENCES

1. Surveys of the Japanese Hydrographic Bureau, *Chart No. 1009, Japan and the Adjacent Seas,* $\frac{1}{3{,}000{,}000}$ (Lat. 35°N).
2. L. G. JACCHIA, Sky and Telescope, **17** (1958), No. 6.
3. I. M. YAÇUNSKI, Uspekhi Fiz. Nauk, **63** (1957), 1, 59–71.